Paper ID: KL-04

Fluid Dynamic Behaviors of Cylindrical Structures

Md. Mahbub Alam
Institute for Turbulence-Noise-Vibration Interaction and Control, Department of Mechanical Engineering and Automation, Shenzhen Graduate School
Harbin Institute of Technology
Shenzhen, China

E-mail: alamm28@yahoo.com; alam@hitsz.edu.cn

Abstract

Multiple cylindrical structures are widely seen in engineering. Flow interference between the structures leads to a very high fluctuating forces, structural vibrations, acoustic noise, or resonance, which in some cases can trigger failure. Recently circular pins in various arrays have been used as fins to enhance the cooling effect. While the enhancement is directly connected to nature of flow around the pins, not much is known about the physics of flow around the pins. The knowledge of flow around two cylinders is insightful for understanding the flow around an array of structures/pins. This paper comprises an in-depth physical discussion of the flow-induced vibration of two circular cylinders in view of the time-mean lift force on stationary cylinders and interaction mechanisms. The gap-spacing ratio T/D is varied from 0.1 to 5 and the attack angle α from 0° to 180° where T is the gap width between the cylinders and D is the diameter of a cylinder. Six interaction mechanisms and five instabilities were observed. While the six interaction mechanisms are connected to six different responses, the five instabilities are responsible for multistable flows. Though a single non-interfering circular cylinder does not correspond to a galloping following quasi-steady galloping theory, two circular cylinders experience violent galloping vibration due to shear-layer/wake and cylinder interaction as well as boundary layer and cylinder interaction. A larger magnitude of fluctuating lift communicates to a larger amplitude vortex excitation.

Keywords: fluid dynamics, structures, forces, instabilities, interactions, flow-induced vibrations.

1. Introduction

Cylindrical structures in a group are frequently seen on land and in the ocean, for example, chimney stacks, tube bundles in heat exchangers, high-rise buildings, harvesting wave and tide energy from ocean, overhead power-line bundles, bridge piers, stays, masts, chemical-reaction towers and offshore platforms. Mutual flow interaction between the structures makes the wake very excited or tranquil depending on the spacing between the structures. The excited wake-enhancing forces in some cases cause a catastrophic failure of the structures. Naturally, it is important to understand the proximity effect on aerodynamics associated with multiple closely spaced cylindrical structures. While much is known of the flow physics around a single isolated cylinder, not much is known of the fluid dynamics around a cylinder neighbored by another. There is no doubt that flow physics around two cylinders is much more complex and more complicated than that around a single cylinder, because of interference between the cylinders [1, 2]. The study of the aerodynamics of two closely separated structures is thus of both fundamental and practical significance. Cross-flow-induced vibration problems are frequently encountered for cylindrical structures such as electric power lines, cooling towers, flow sensor tubing, cables of suspension bridges, etc. The resulting vibrations depend strongly on cylinder configuration (relative to flow), pitch spacing, cylinder diameters and flow conditions. The cross-flow-induced vibration is the most important problem in various fields, and is known to have caused many failures in various industrial components.

Time-mean drag and lift forces acting on two staggered cylinders have been examined in the literature (e.g. [3-5]), with most of the emphasis being on the downstream cylinder. Only a few studies have reported force measurements for the upstream cylinder [6-9]. Furthermore, fluctuating force measurements in the literature are very scant, though the fluctuating lift and drag forces acting on structures are a major cause of the fatigue failure of the structures and are used for predicting flow-induced responses. Most literature sources are connected to

one of the three arrangements, tandem ($\alpha = 0°$) or side-by-side ($\alpha = 90°$) or staggered ($0° < \alpha < 90°$). See Fig. 1 for definitions of symbols. Furthermore, flow classifications in the literature are based on either theoretical treatment [10], or experimental measurement of forces, *St* and pressure (e.g. [4]) or flow visualization image (e.g. [11]).

The instability of slender structures has received the attention of many scientists during decades [12-15]. One of the reasons for such studies is the fact that buildings and other slender structural elements are built more and more frequently using new techniques that involve weight-saving materials (thus reducing the overall stiffness) and innovative cross-sectional geometries. In consequence, when designing certain structures such as particularly high and slender buildings, one may find that critical velocities of aeroelastic instabilities such as vortex-induced excitation and galloping are within the design wind speed.

Practically no structure is perfectly rigid, hence it is worthy to gain physical insight into the flow-induced response of the structure. Bokaian and Geoola [16] investigated the case of two identical cylinders in tandem and staggered arrangements where the downstream one was fixed and the upstream one both-end-spring-mounted, allowing both ends to vibrate at the same amplitude (two-dimensional model) in the cross-flow direction only. They reported galloping vibration generated at a spacing ratio of $T/D < 0.8$ ($\alpha = 25°$), $T/D \leq 0.75$ ($\alpha = 0°$) and vortex excitation (VE) at other T/D and α. Bokaian and Geoola [17] also investigated the other case where the upstream cylinder was fixed and the downstream one was free to oscillate. Depending on T/D, the cylinder exhibited either only galloping ($T/D = 0.59$, $\alpha = 0°$) or only VE ($T/D > 1.5$, $\alpha = 0°$) or a combined VE and galloping ($T/D > 0.5$, $\alpha = 0°$), or a separated VE and galloping ($1.0 \leq T/D \leq 1.5$). Note that the vibration always occurs at the natural frequency f_n of the cylinder. The VE corresponded to vibration occurring near the reduced velocity U_r ($= U_\infty/f_nD$, U_∞ is the free-stream velocity) where the natural vortex-shedding frequency f_v is close to f_n. On the other hand, the galloping vibrations persist for higher U_r corresponding to a higher f_v than f_n. In Bokaian and Geoola [16-17], the investigated ranges of T/D, α and mass-damping factor $m^*\zeta$ were 0.09 ~ 4, 0° ~ 70° and 0.018 ~ 0.2, respectively, where m^* is the mass ratio and ζ is the damping ratio.

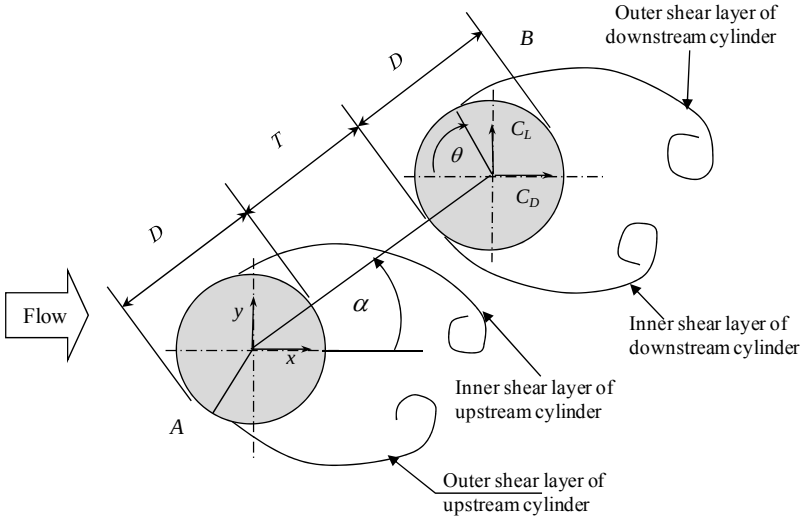

Fig. 1. Arrangement of cylinders and definitions of symbols.

Laneville and Brika [18] coupled two identical cylinders ($T/D = 7 \sim 25$, $m^*\zeta = 0.00007$) mechanically by thin wires, allowing them to vibrate in in-phase and out-of-phase mode. They found that the response of the cylinder is more complex and dependent on the coupling mode. Huera-Huarte and Bearman [19] conducted experiments on flow-induced responses of two tandem cylinders for $L/D = 1$ to 3 at $m^*\zeta = 0.043$. The upstream cylinder experienced larger vibrations than the rear one for small gap distances at small U_r, when the shedding frequency was close to its natural frequency. The downstream cylinder exhibited galloping with large amplitudes at high U_r for the largest gap separations.

Alam and Kim [20] and Kim et al. [21] conducted a systematic investigation on flow-induced response characteristics of two circular cylinders at $\alpha = 0° \sim 90°$, $T/D = 0.1 \sim 3.2$. Dependence of vibration-amplitude-to-diameter ratio a/D on reduced velocity U_r was examined.

The objectives of this study were to (i) classify possible interaction mechanisms and instability for two stationary rigid cylinders, and (ii) correlate interaction mechanisms, lift forces and flow-induced responses of

the cylinders mounted elastically. The possible range of α = 0° ~ 180° was considered with T/D = 0.1 ~ 5.0. Flow-induced response results are incorporated from literature published by the current author and others.

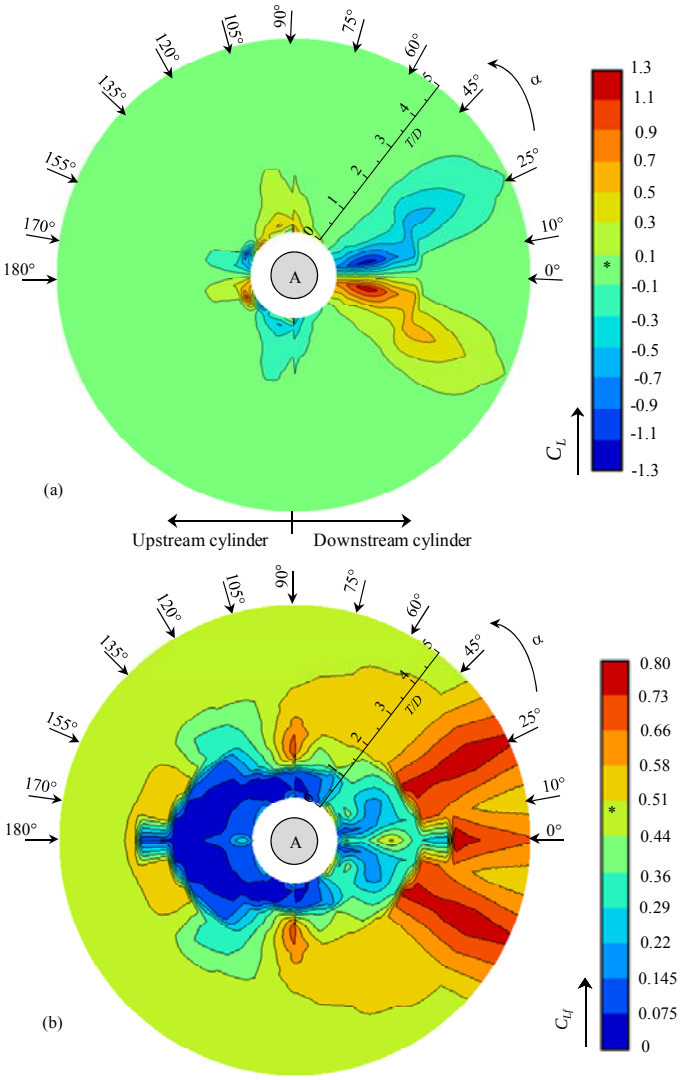

Fig. 2. Contour maps of (a) time-mean lift coefficient C_L and (b) fluctuating lift coefficient C_{Lf} of cylinder *B*. [1]. Points marked by '*' denote values of coefficients of an isolated cylinder.

2. Experimental details

Fluid force measurements were conducted in a closed-circuit wind tunnel with a 2.2-m-long test section of 0.3 m in width and 1.2 m in height at Kitami Institute of Technology. Two circular cylinders of the same diameter D = 49 mm, made of brass, spanned horizontally across the test section width. The free-stream velocity, U_∞, was 17 m/s, resulting in Reynolds number Re ($\equiv U_\infty D/\nu$) = 5.5 × 10^4, where ν is the kinematic viscosity of air. The flow non-uniformity was within ± 0.2% (rms) inside the central cross-sectional area of 0.24 m × 0.95 m in the test section, and the longitudinal turbulence intensity was less than 0.5% in the absence of the cylinders. A schematic diagram of the cylinder arrangement appears in Fig. 1, along with the definitions of symbols. The Cartesian coordinate system was defined such that the origin was at the center of Cylinder *A*, with the *x*- and y-axis along the streamwise and lateral directions, respectively.

Fluid forces were measured over a small spanwise length of the cylinders using load cells. Measurements were done for α = 0° ~ 180°, T/D = 0.1 ~ 5. Tuning of T/D was T/D = 0.1, 0.2, 0.3, 0.5, 0.6, 0.7, 0.8, 0.9, 1.1, 1.2, 1.5, 1.8, 2.1, 2.4, 2.7, 3.0, 3.5, 4.0, 4.5 and 5.0.

Flow visualization was carried out in a water channel with a 300 × 350 mm working section and 1.5 m in length. Two circular tubes with identical diameters of 20 mm were used. The Reynolds number in the water channel experiment was 350. The flow was visualized by using the hydrogen bubble technique, involving a platinum wire of 0.02 mm in diameter.

3. Results and discussion

3.1. Fixed cylinders

Lift forces

Time-averaged lift coefficient (C_L) and fluctuating (rms) lift coefficient (C_{Lf}) are measured for the whole ranges of α and T/D mentioned in section 2. Contours of time-averaged lift coefficient (C_L) and fluctuating (rms) lift coefficient (C_{Lf}) measured on the C_L and C_{Lf} in a T/D - α plane are presented in Fig. 2. In the scale bars, the color or the range marked by black '*' indicates the value of a single isolated cylinder. The result can be described with reference to Fig. 1 in which Cylinder A is fixed, and traversing of Cylinder B is done with variations of the two parameters T/D and α, which suffice to determine the possible arrangement of the two cylinders. It may be noted that Cylinder B acts as the downstream cylinder for $|\alpha| < 90°$ and the upstream cylinders for $|\alpha| > 90°$, i.e. the left and right sides of a contour map show the values of coefficient of the upstream and downstream cylinders, respectively. At the peripheries of the middle and outer circles, the values of T/D are 0.0 and 5.0, respectively. Upward (+ve y-direction) C_L is considered as positive.

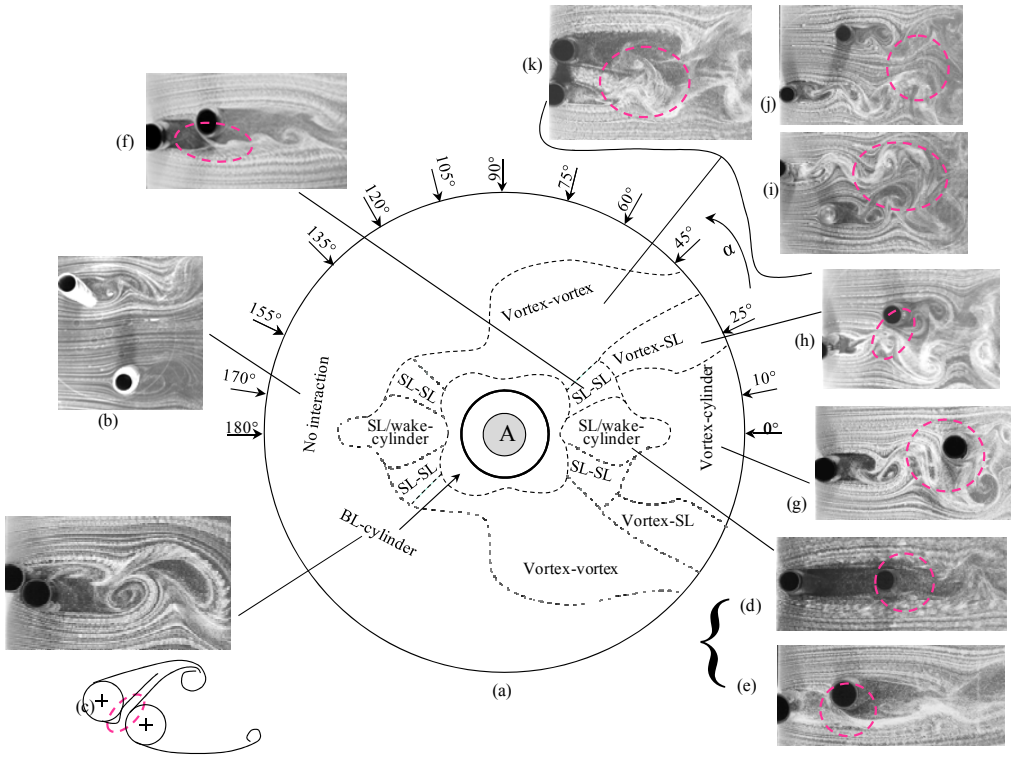

Fig. 3. Interaction regimes in T/D - α plane. SL : shear layer, BL : boundary layer.

The C_L in the downstream region (right half) is highly sensitive to T/D and α; however, that in the upstream region (left half) retains single-cylinder values except for $|\alpha| = 135°$-$180°$, $T/D < 0.4$ - 1.0, and $|\alpha| = 90°$ - 135°, $T/D < 1.3$ - 0.4. The C_L around the cylinder for $T/D < 0.5$ varies greatly with change in α from 0° to 360°. The minimum (most negative) values of $C_L = -1.03$ and - 1.15 ~ - 1.25 occur at $\alpha = 155°$, $T/D = 0.3$ and $\alpha = 10°$, $T/D = 0.8 \sim 1.1$, respectively. At the respective conjugate positions, C_L increases to a maximum. On the other hand, C_{Lf} is extremely small for smaller spacing, i.e., $T/D < 2$ - 3 depending on α (Fig. 2b) and remarkably high for α = - 35° to 35°, $T/D > 2.5$ - 3.0. Hence the interference between the cylinders not only has a negative effect by

increasing forces, but also a positive effect by reducing forces on the cylinder. Its effect, however, depends on α and *T/D*. It is expected that at different values of *T/D* and α, interaction mechanisms between the cylinders will be different, hence C_L and C_{Lf} are strong functions of *T/D* and α.

Flow-structure interaction

When one cylinder is neighbored by another, the two cylinders may be connected to or interacted by boundary layers, shear layer, vortex and wake. Therefore it is possible that a cylinder may experience complex interaction mechanisms where cylinder, boundary layer, shear layer, vortex and wake are the five physical interacting parameters. Based on interaction mechanisms, the whole region of α and *T/D*, can be classified into six regimes as illustrated in Fig. 3, viz, boundary-layer (BL) and cylinder interaction regime, shear-layer/wake and cylinder interaction regime, shear-layer (SL) and shear-layer (SL) interaction regime, vortex and cylinder interaction regime, vortex and shear-layer (SL) interaction regime, vortex and vortex interaction regime. The flow structures given explicate the difference between the interactions.

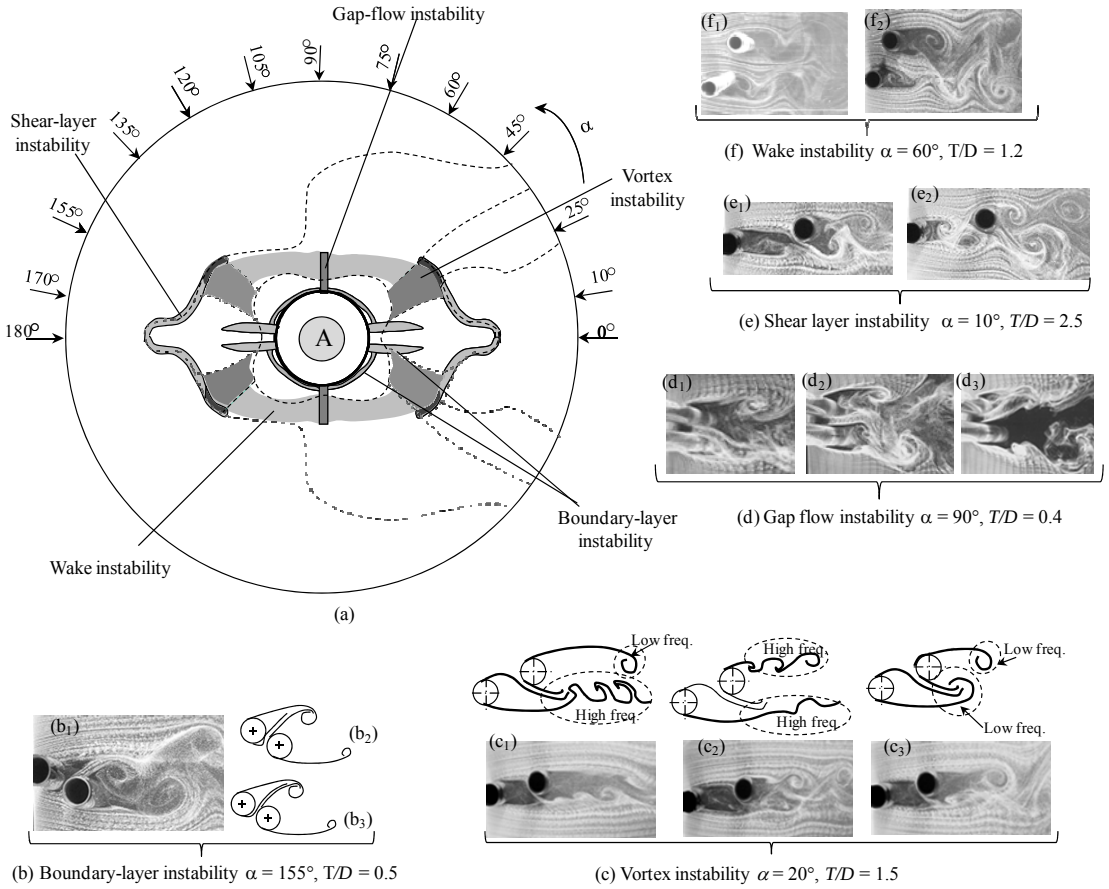

Fig. 4. (a) Types of instability and their regimes. (b-f) Multistable flow caused by the instabilities.

Flow instability

When two cylinders interact each other in the above six mechanisms, instabilities were observed in the boundary-layer, vortex, gap-flow, shear-layer and wake. The regimes where the instabilities appear are shadowed as in Fig. 4. The boundary-layer instability occurring when *T/D* is small causes formation and burst of a separation bubble (Fig. 4b_2, b_3), responsible for bistable flow. Hence a discontinuous jump/drop in lift or drag forces is afoot. When the outer shear layers of the two cylinders shed vortices at different frequencies at an intermediate α, vortex instability may result in lock-in between the vortices from the two sides, generating a tristable wake of low-high, high-high and low-low frequencies (Fig. 4c). Being very unstable, the gap flow at α

≈ 90° switches from a side to the other, engendering bistable or tristable flow (Fig. 4d). While the gap flow is biased downward (Fig. $4d_1$), it becomes straight (Fig. $4d_2$) and then swerves upward (Fig. $4d_3$). Mutual switch between reattachment (Fig. $4e_1$) and coshedding flow (Fig. $4e_2$) occurs due to instability of the upstream-cylinder shear layer when two cylinders are nearly tandem ($\alpha < 25°$). For larger α, the two wakes may have the different vortex frequencies (Fig. $4f_2$) but intermittently they become locked-in having the same frequency of vortices (Fig. $4f_1$).

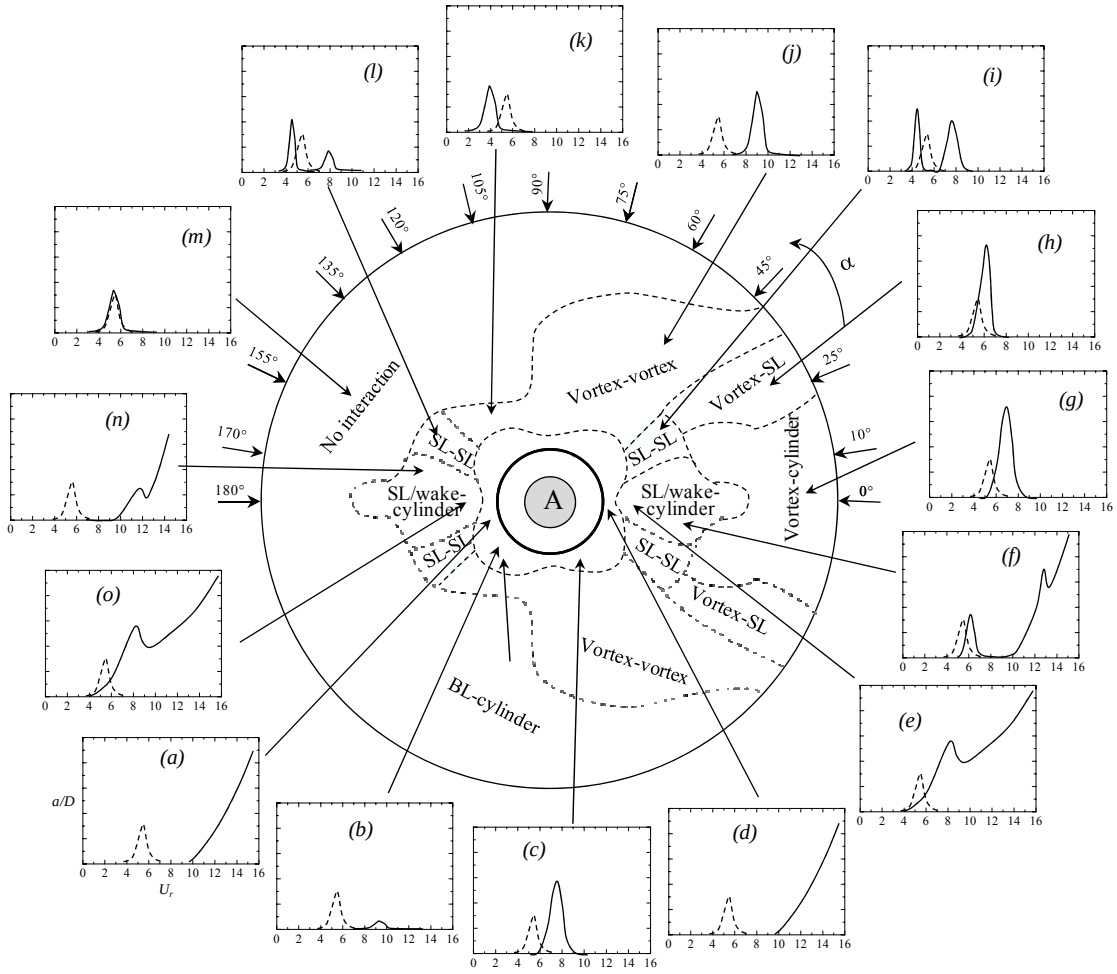

Fig. 5. Nature of flow-induced vibration responses at different interaction regimes. Dashed line represents a single isolated cylinder response. The vertical and horizontal axes of the response graphs are the vibration amplitude ratio a/D and reduced velocity U_r ($= U_\infty/f_n D$). The response curves are based on the results in [17-18 20].

3.2. Flexible cylinders

Flow-induced vibrations

How the interactions affect flow-induced instability of the two cylinders - compared to a single isolated (non-interfering) cylinder - is of great interest to researchers in science and engineering. This section includes an overview of flow-induced vibration results for two elastically mounted cylinders. The detailed results of cylinder responses at different interaction regimes are presented in Fig. 5. While the vertical axis of the response curves represents the vibration amplitude a normalized by D, the horizontal axis is U_r. The response curves were incorporated from Refs. [16-17], and Alam and Kim [20]. The dashed line in the response graphs stands for single isolated cylinder response, insinuating VE at $U_r \approx 5.4$ (≈1/St = 1/0.186). While both cylinders experience divergent galloping vibration for $U_r > 10$ at $0 < \alpha < 25°$ (Fig. 5a, d) in the boundary layer and cylinder interaction regime, they experience VE between $U_r = 7$ to 10 for $25° < \alpha < 155°$ (Fig. 5b, c). For the latter case, the downstream cylinder vibration amplitude is larger than the upstream one. Divergent violent vibrations of

both cylinders are generated in the regime of shear-layer/wake and cylinder interaction (Fig. 5e, f, n, o). VE and galloping are combined at smaller *T/D* (Fig. 5e, o) and separated for larger *T/D* (Fig. 5f). High amplitude VE is afoot in the regimes of vortex and cylinder interaction (Fig. 5g) and vortex and shear-layer interaction (Fig. 5h), where C_{Lf} on stationary cylinders is high (Fig. 2b). In the SL and SL interaction regime, VE occurs at two regimes of U_r (Fig. 5i, l). Each cylinder sheds vortices at two frequencies [22], hence experiences two VE. In the vortex and vortex interaction regime, VE intervenes at a high U_r for the downstream cylinder (Fig. 5j) and at a low U_r for the upstream cylinder (Fig. 5k). This is due to the fact that the downstream and upstream cylinders generally shed vortices at a low and at a high frequency, respectively. The no interaction regime corresponds to VE at the same U_r as that of a single cylinder (Fig. 5m).

It is worth mentioning that a larger C_{Lf} (Fig. 2b) corresponds to larger amplitude VE (Fig. 5c, g, h). The most striking feature is that divergent galloping vibration is generated at shear layer/wake and cylinder interaction (Fig. 5e, f, n, o) and at boundary layer and cylinder interaction (Fig. 5a, d) regimes where there is a large variation in C_L in the cross-flow direction (Fig. 2a). Based on galloping theories it is an acknowledged fact that galloping is not generated on an axis-symmetric body, e.g. a circular cylinder. Hence the question arises, why do two circular cylinders in close proximity experience galloping? In the regimes of boundary layer and cylinder interaction as well as shear -layer/wake and cylinder interaction, the two cylinders are connected by boundary layer or shear layer, and the combined shape of the two cylinders is not longer axis symmetric, hence the two cylinders may be prone to generating galloping vibrations. Furthermore, due to having non-uniform velocity between the cylinders, the downstream cylinder is again not axis symmetric with respect to local approaching flow. In other words, the galloping generation for two circular cylinders at close proximity is not violating the galloping theories. Details of the instability mechanism are discussed in the next section with reference to the lift force and interaction mechanisms.

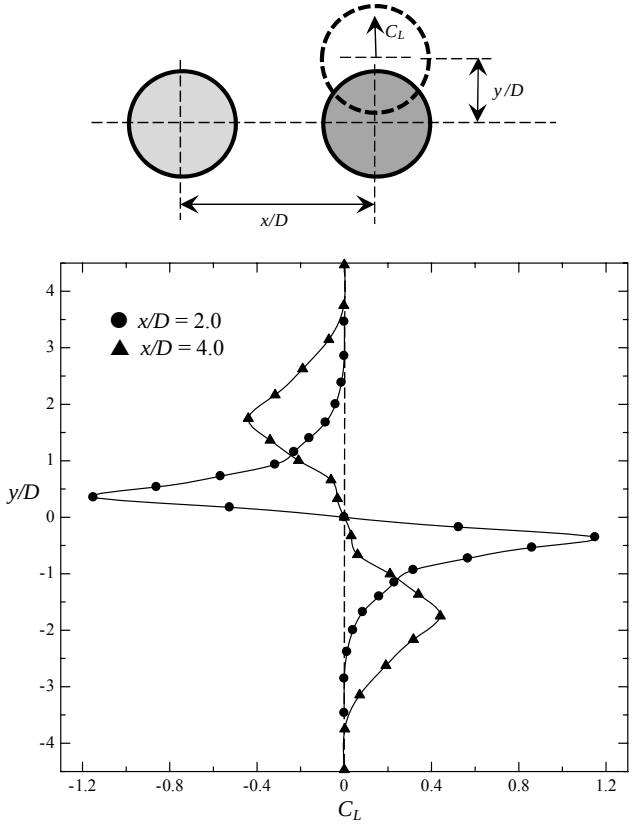

Fig. 6. Variations in C_L with *y/D* at *x/D* = 2.0 and 4.0.

Galloping mechanism

Figure 6 shows C_L variation with change in *y/D* at *x/D* = 2 and 4. C_L is maximum and minimum at *y/D* = - 0.4 and 0.4, respectively for *x/D* = 2 and at *y/D* = - 1.8 and 1.8 for *x/D* = 4. These two *y/D* values correspond to the locations of positive and negative peaks in the C_L contour map (Fig. 3a). The figure suggests that when the cylinder position is below the center line (*y/D* = 0), C_L is in an upward direction; and when the cylinder position

is above the center line, C_L is in a downward direction. Now it is possible to get $\partial C_L / \partial(y/D)$. Figure 7 shows how $\partial C_L / \partial(y/D)$ varies with *y/D*. It is clear that the system is stable for *y/D* = -0.4 ~ 0.4 and unstable for | *y/D*| > 0.4 (Fig. 7a). In the former region, our intuition is confirmed: in the case of the tandem cylinder (*y/D* = 0), when the downstream cylinder is displaced in the transverse direction away from *y/D* = 0 line, there is a restoring lift force that is acting to return the cylinder to its original position (see Fig. 6). Hence quasi-steady arguments, as used in galloping theory, suggest stability of the downstream cylinder rather than instability. Galloping type response however occurs at *y/D* = - 0.4 ~ 0.4 (Fig. 5). Why and how? At *y/D* = 0, C_L = 0 (Fig. 6), there is no force to displace the cylinder in a transverse direction. But for *y/D* ≠ 0, $C_L \neq 0$, i.e., a force exists to displace the cylinder from its neutral position. Cylinder motion is thus generated, though displacement may be very small. It does not matter in which direction the displacement occurs.

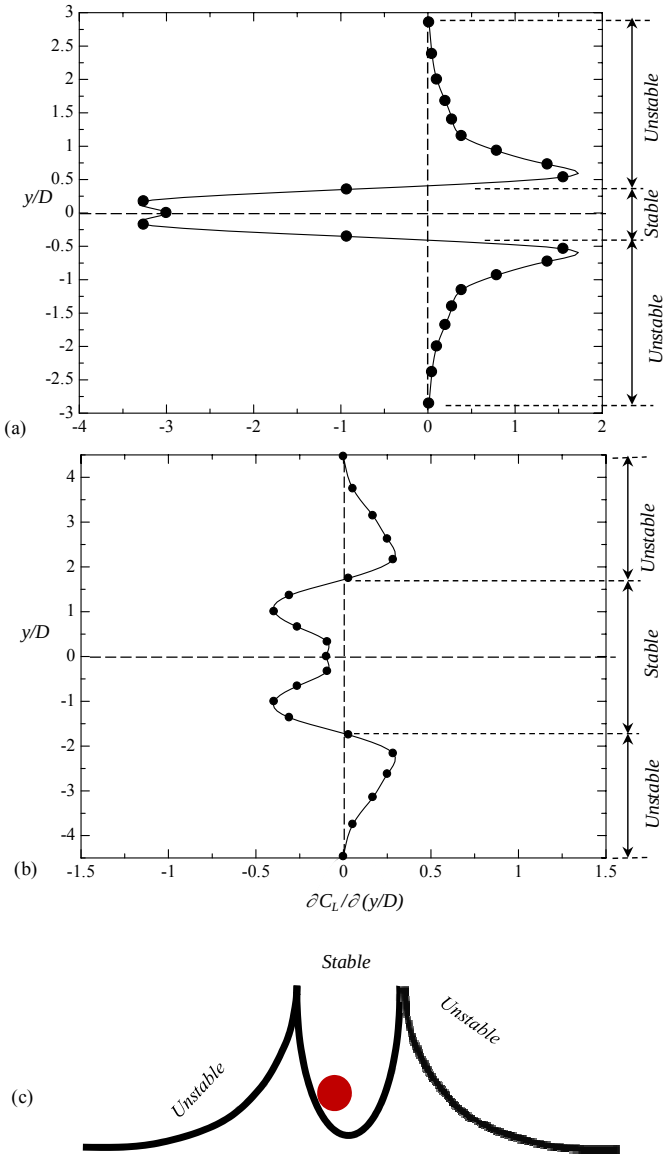

Fig. 7. Dependence of lift-force gradient $\partial C_L / \partial(y/D)$ on *y/D* at (a) *x/D* = 2.0 and (b)) *x/D* = 2.0 . (c) Sketch showing stability and instability. In fact, the $\partial C_L / \partial(y/D)$ variation corresponds to an extremely slow motion, i.e., f_n = very low.

The question that now arises is how an initial displacement for *y/D* = 0 occurs. Indeed, *y/D* = 0 is the critical geometry between staggered configurations of *y/D* = 0+ and *y/D* = 0-. For *y/D* = 0+, only the upper shear layer of the upstream cylinder reattaches onto the upper surface of the downstream cylinder; for *y/D* = 0-, only the lower shear layer of the upstream cylinder reattaches onto the lower surface of the downstream cylinder. Hence,

for y/D = 0, the upper and lower shear layers of the upstream cylinder reattach alternately onto the upper and lower surfaces of the downstream cylinder, respectively, especially for T/D smaller than critical spacing. This alternating reattachment generates fluctuating forces to displace the cylinder. When the cylinder is slightly displaced (Fig. 8a), the reattached shear layer is in a hesitating position, critically hovering to go on the upper side or the lower side. Instability is thus generated. For a cylinder spacing larger than critical, the oncoming vortex also has two options of where to go, on the upper side and lower side (Fig. 8b). This hesitation is responsible for generating the instability.

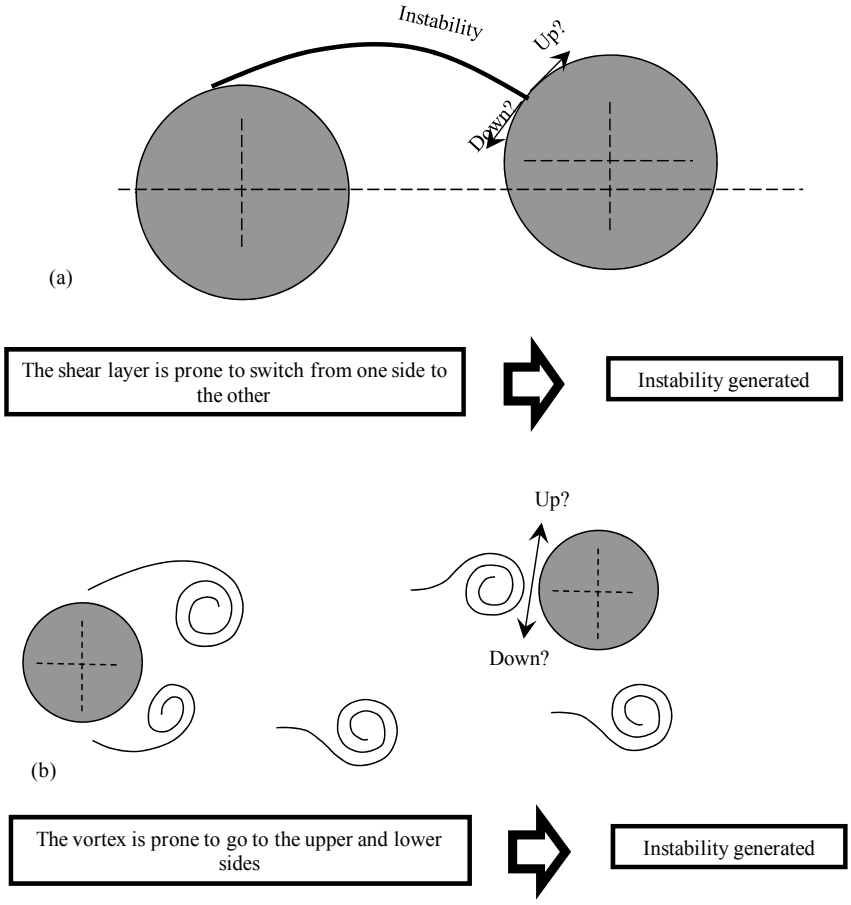

Fig. 8. Instability generation for (a) T/D < critical, (b) T/D > critical.

4. Conclusions

Time-mean lift, fluctuating lift, flow structures and the flow-induced responses of two circular cylinders are hooked up with mechanisms of interaction between the cylinders for all possible arrangements. The current investigation has led to the conclusions below.

Fluid dynamics around two cylinders is classified into six based on how the two cylinders interact with each other. The six occur at six different interaction regimes, namely, boundary layer and cylinder interaction regime; SL/wake and cylinder interaction regime; SL and SL interaction regime; vortex and cylinder interaction regime; vortex and SL interaction regime; and vortex and vortex interaction regime. Each of them has different traits and is connected to a different flow-induced response. While the boundary layer and cylinder interaction intensifies the lift force and generates galloping vibration, the SL/wake and cylinder interaction make changes in lift forces briskly with α or y/D, reduces fluctuating lift and generates both VE and galloping vibration. Two VEs occur at two different reduced velocities in the SL and SL interaction regime. Both vortex and cylinder interaction and vortex and shear layer interaction causes extensively high fluctuating lift, generating relatively high amplitude VE. The VE-reduced velocity is slightly higher for the vortex and cylinder interaction than for the vortex and shear layer interaction. Vortex and vortex interaction results in a slightly higher fluctuating lift and generates VE

only.

Though a single non-interfering circular cylinder does not experience galloping, two circular cylinders incur violent galloping vibration due to SL/wake and cylinder interaction as well as boundary-layer and cylinder interaction. A stronger fluctuating lift corresponds to a larger amplitude VE.

5. Acknowledgments

The author wishes to acknowledge supports given to him from Shenzhen Government through grant CB24405004 and from China Govt through '1000-young-talent-program'.

6. References

[1] M.M. Alam, and J.P. Meyer, "Two Interacting Cylinders in Cross Flow", *Physical Review E*, Vol. 84, 056304, pp. 16, 2011.

[3] J. Price, "The Origin and Nature of the Lift Force on the Leeward of Two Bluff Bodies", *Aeronautical Quarterly,* Vol. 26, pp. 154–168, 1976.

[4] M.M. Zdravkovich, and D.L. Pridden, "Interference between Two Circular Cylinders; Series of Unexpected Discontinuities", *Journal of Industrial Aerodynamics*, Vol. 2, pp. 255-270, 1977..

[5] S.J. Price, and M.P. Paidoussis, "The Aerodynamic Forces acting on Groups of Two and Three Circular Cylinders when Subject to a Cross-Flow", *Journal of Wind Engineering and Industrial Aerodynamics,* Vol. 17, pp. 329-347, 1984.

[6] M.M. Alam, M. Moriya, K. Takai, and H. Sakamoto, "Fluctuating Fluid Forces acting on Two Circular Cylinders in a Tandem Arrangement at a Subcritical Reynolds number", *Journal of Wind Engineering and Industrial Aerodynamics*, Vol. 91, pp. 139–154, 2003.

[7] M.M. Alam, M. Moriya, and H. Sakamoto, 2003 "Aerodynamic characteristics of two side-by-side circular cylinders and application of wavelet analysis on the switching phenomenon", *Journal* of *Fluids and Structures*, Vol. 18, pp. 325-346.

[8] Z. Gu, and T. Sun, "On Interference between Two Circular Cylinders in Staggered Arrangement at High Subcritical Reynolds Numbers", *Journal of Wind Engineering and Industrial Aerodynamics,* Vol. 80, pp. 287-309, 1999.

[9] M.M. Alam, H. Sakamoto, and Y. Zhou, "Determination of Flow Configurations and Fluid Forces acting on Two Staggered Circular Cylinders of Equal Diameter in Cross-Flow," *Journal* of *Fluids and Structures*, Vol. 21, pp. 363-394, 2005.

[10] M.M. Zdravkovich, "The Effects of Interference between Circular Cylinders in Cross Flow", *Journal* of *Fluids and Structures*, Vol. 1, pp. 239-261, 1987.

[11] I. Peschard, and P. Le Gal, "Coupled Wakes of Cylinders", *Physical Review Letters*, Vol. 77, pp. 3122–3125, 1996.

[12] G. Parkinson, and J. Smith, "The Square Cylinder as an Aeroelastic Non-Linear Oscillator", *Journal of Mechanics and. Applied mathematics*, Vol.17, pp. 225–239, 1964.

[13] M. Novak, "Aeroelastic Galloping of Prismatic Bodies", *Journal of Engineering Mechanics Division, Proc.* ASCE, Vol. 9, pp. 115–142, 1969.

[14] E. Simiu, and R.H. Scanlan, "Wind Effects on Structures. Fundamentals and Applications to Design, Wiley, New York, 1996.

[15] M. Novak, "Galloping Oscillations of Prismatic Structures", *Journal of Engineering Mechanics Division, Proc.* ASCE, Vol. 98, pp. 27–46, 1972.

[16] A. Bokaian, and F. Geoola, "Proximity-Induced Galloping of Two Interfering Circular Cylinders", *Journal of Fluid Mechanics*, Vol. 146, pp. 417-449, 1984.

[17] A. Bokaian, and F. Geoola, "Wake-Induced Galloping of Two Interfering Circular Cylinders. *Journal of Fluid Mechanics*, Vol. 146, pp. 383-415, 1984.

[18] A. Laneville, and D. Brika, "The Fluid and Mechanical Coupling between Two Circular Cylinders in Tandem Arrangement", *Journal* of *Fluids and Structures*, Vol. 13, 967-986, 1999.

[19] F.J. Huera-Huarte, and P.W. Bearman, "Vortex and Wake-Induced Vibrations of a Tandem Arrangement of Two Flexible Circular Cylinders with Near Wake Interference", *Journal* of *Fluids and Structures*, Vol. 27, pp. 193 – 211, 2011.

[2] M.M. Alam, Y. Zhou, and X.W. Wang, "The Wake of Two side-by-side Square Cylinders", *Journal of Fluid Mechanics*, Vol. 669, pp. 432-471, 2011.

[20] M.M. Alam, and S. Kim, "Free Vibration of Two Identical Circular Cylinders in Staggered Arrangement", *Fluid Dynamic Research*, Vol. 41, 035507, 17pp, 2009..

[21] S. Kim, M.M. Alam, H. Sakamoto, and Y. Zhou, "Flow-Induced Vibrations of Two Circular Cylinders in Tandem Arrangement, Part 1: Characteristics of Vibration", *Journal of Wind Engineering and Industrial Aerodynamics,* Vol. 97, pp. 304-311, 2009.

[22] M.M. Alam, and H. Sakamoto, "Investigation of Strouhal Frequencies of Two Staggered Bluff Bodies and Detection of Multistable Flow by Wavelets", *Journal* of *Fluids and Structures*, Vol. 20(3), pp. 425-449, 2005.